Available online at www.sciencedirect.com
SCIENCE DIRECT
Journal of Power Sources 158 (2006) 524–528
JOURNAL OF POWER SOURCES
www.elsevier.com/locate/jpowsour

Stannum doping of layered $LiNi_{3/8}Co_{2/8}Mn_{3/8}O_2$ cathode materials with high rate capability for Li-ion batteries

Jiangang Li [a,b], Xiangming He [b,*], Rusong Zhao [a], Chunrong Wan [b], Changyin Jiang [b], Dingguo Xia [c], Shichao Zhang [d]

[a] *School of Material and Chemical Engineering, Beijng Institute of Petrochemical Technology, Beijing 102617, PR China*
[b] *Materials Chemistry Lab, Institute of Nuclear and New Energy Technology, Tsinghua University, Beijing 100084, PR China*
[c] *College of Energy and Environmental Engineering, Beijing University of Technology, Beijing 100022, PR China*
[d] *School of Material Science and Engineering, Beihang University, Beijing 100083, PR China*

Received 11 June 2005; received in revised form 20 August 2005; accepted 24 August 2005
Available online 8 November 2005

Abstract

Sn doped lithium nickel cobalt manganese composite oxide of $LiNi_{3/8}Co_{2/8}Mn_{3/8-x}Sn_xO_2$ ($0 \le x \le 0.10$) was synthesized by stannum substitute of manganese to enhance its rate capability at first time. Its structure and electrochemical properties were characterized by X-ray diffraction (XRD), SEM, cyclic voltammetry (CV), galvanostatic intermittent titration technique (GITT) and charge/discharge tests. $LiNi_{3/8}Co_{2/8}Mn_{3/8-x}Sn_xO_2$ had stable layered structure with α-$NaFeO_2$ type as x up to 0.05, meanwhile, its chemical diffusion coefficient D_{Li} of Li-ion was enhanced by almost one order of magnitude, leading to notable improvement of the rate capability of $LiNi_{3/8}Co_{2/8}Mn_{3/8}O_2$. The compound of $x = 0.10$ showed the best rate capability among Sn doped samples, but its discharge capacity reduced markedly due to secondary phase Li_2SnO_3 and increase of cation-disorder. The compound with $x = 0.05$ showed high rate capability with initial discharge capacity in excess of 156 mAh g^{-1}. It is a promising alternative cathode material for EV application of Li-ion batteries.

Keywords: Li-ion batteries; $LiNi_{3/8}Co_{2/8}Mn_{3/8}O_2$; Stannum doping; High rate capability; Diffusion coefficient

1. Introduction

Rechargeable Li-ion battery, with high energy density and long life, has been applied successfully in portable electronic appliances such as mobile telephones and laptop computers, and is also considered to be a promising alternative for application in electric vehicles (EV) and hybrid electric vehicles (HEV) [1–6]. But conventional $LiCoO_2$ has the shortage of cost and thermal safety problems, significant efforts have been made by many groups in recent years to develop a cheaper, higher capacity, and safer cathode material to replace $LiCoO_2$. $LiMn_2O_4$, $LiMnO_2$, $LiNiO_2$, $LiFePO_4$, etc. and their derivatives, have been studied extensively as possible substitution [1–4,6].

$LiNi_{1/2}Mn_{1/2}O_2$ is considered to be one of very promising cathode materials because it is cheaper, higher capacity (150–160 mAh g^{-1}) and thermally safer than $LiCoO_2$ [7,8]. If its impedance could be suppressed to a low level, the large application in EV or HEV is possible. To accomplish this object, a large amount investigation about its derivatives $Li(Ni_{0.5-x}Mn_{0.5-x}M_{2x})O_2$ (M = Co, Al, Ti; $x = 0$, 0.025) [9], $Li(Ni_xCo_{1-2x}Mn_x)O_2$ ($x = 1/2$, 3/8) [10], $xLiNi_{1/2}Mn_{1/2}O_2 \cdot (1-x)\ Li_2TiO_3$ ($x = 0.95$) [11] and $Li(Ni_{1/3}Co_{1/3}Mn_{1/3})O_2$ [12], have been carried out, and the results show that cobalt doping can improve the electronic conductivity and cycleability obviously [9], but the thermal stability declines as Co content increases [10].

Considering electrochemical performances and thermal safety, lithium nickel cobalt manganese composite oxide $LiNi_{3/8}Co_{2/8}Mn_{3/8}O_2$ has been investigated in our previous studies, showing good electrochemical performance [13,14].

In this study, novel layered $LiNi_{3/8}Co_{2/8}Mn_{3/8-x}Sn_xO_2$ ($0 \le x \le 0.10$) cathode materials were synthesized by introduc-

* Corresponding author. Tel.: +86 10 89796073; fax: +86 10 89796031.
E-mail addresses: hexm@tsinghua.edu.cn, hexiangming@tsinghua.org.cn (X. He).

0378-7753/$ – see front matter © 2005 Elsevier B.V. All rights reserved.
doi:10.1016/j.jpowsour.2005.08.026

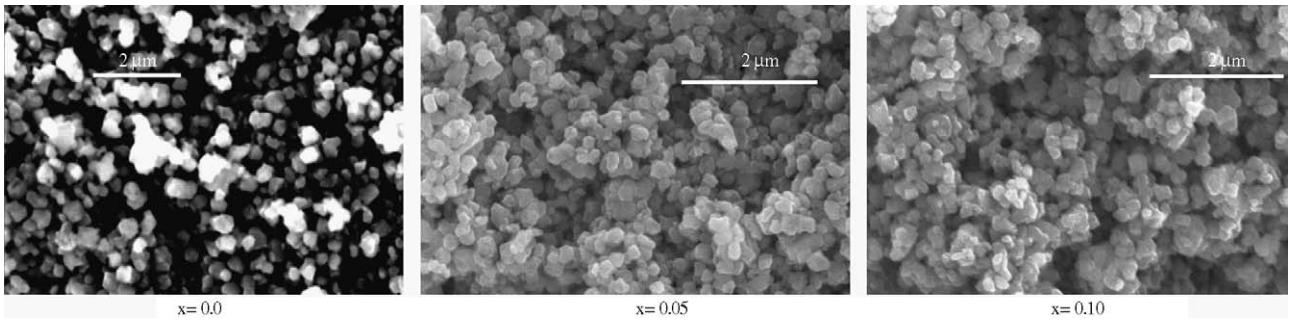

Fig. 1. SEM images of $LiNi_{3/8}Co_{2/8}Mn_{3/8-x}Sn_xO_2$.

ing stannum metal elements to improve the rate capability. The mechanism and electrochemical properties were investigated, and the experiment results showed that Sn^{4+} substitution for Mn^{4+} could improve its rate capability markedly.

2. Experimental

$LiNi_{3/8}Co_{2/8}Mn_{3/8-x}Sn_xO_2$ ($x = 0.00, 0.025, 0.05, 0.10$) samples were prepared as follows. Firstly, $Ni_{3/8}Co_{2/8}Mn_{3/8-x}(OH)_{2-2x}$ precursors were prepared using the co-precipitation method described in [7–10], then a stoichiometric mixture of $LiOH{\cdot}H_2O$, $Ni_{3/8}Co_{2/8}Mn_{3/8-x}(OH)_{2-2x}$ and SnO_2 were ground thoroughly and preheated at 600 °C in air for 5 h. The obtained powders were reground thoroughly, pressed into pellets, and heated at 900 °C in air for 5 h. After quenching in liquid N_2 [15,16], the resulting powders were ground and 600-mesh-sieved, then identified by M21X X-ray diffractometer using Cu Kα radiation, STEREOSCAN-200 scanning electron microscope and CHEMBET-3000 chemical absorption analyzer.

The electrochemical characteristics of the powders were tested at room temperature using Solartron 1470 multi-channel battery test analyzer and Swagelock cell with three electrodes. Positive electrode was prepared by mixing of 85 wt.% active material, 10 wt.% acetylene black and 5 wt.% PVDF binder in *N*-methyl-pyrrolidinone as solvent, then cast the resulting paste on an aluminum foil and dried for 1 h at 110 °C. After that the working electrode was punched out with 0.5 cm^2 geometric area, pressed and vacuum dried at 120 °C for 20 h. The typical active material weight is 6 mg. The lithium metal was used as the negative electrode and counter electrode. Celgard 2400 microporous membrane was used as the separator. The electrolyte was 1 M $LiPF_6$ in EC/DMC/EMC (1:1:1 by volume) solution. The entire cells were assembled in the argon-filled glove box (M-Braun). The cells were charged/discharged for 5 cycles at a constant current of 30 mA g^{-1} in the voltage range 4.4 and 2.5 V. Then the rate capability of the cells were tested by charging to 4.4 V using a constant current of 30 mA g^{-1} and discharging to 2.5 V under the constant currents of 23, 58, 116, 232, 464 mA g^{-1}, respectively.

The cyclic voltammetry tests were conducted in the voltage range 4.4 and 2.5 V at a scan rate of 0.1 mV s^{-1}. The chemical diffusion coefficients of Li-ion, D_{Li}, were tested using GITT method at current pulses of 0.78 mA during 150 s (each one corresponding to $y = 0.02$ in $Li_yNi_{3/8}Co_{2/8}Mn_{3/8-x}Sn_xO_2$) followed by a potential relaxation step at open circuit until the cell voltage variation was less than 4 mV h^{-1}.

3. Results and discussion

SEM images of the powders with different amount of Sn dopant show that no morphological changes occur as Sn dopant increases. The typical image of samples with $x = 0.00$, 0.05 and 0.10 are shown in Fig. 1. All samples have fine, uniform particle sizes ranging from 150 to 300 nm.

The specific surface areas measured by BET are 3.25, 3.19, 3.29 and 3.22 $m^2\ g^{-1}$ for the samples of $x = 0.00$, 0.025, 0.05 and 0.10, respectively. These results are identical to the SEM analysis of samples.

Fig. 2 shows the XRD patterns of $LiNi_{3/8}Co_{2/8}Mn_{3/8-x}Sn_xO_2$ ($x = 0.025$, 0.05, 0.10) samples. All of peaks can be indexed based on the α-$NaFeO_2$ structure, no impurity phases peaks are observed in the range of $0 \le x \le 0.05$. However, secondary phase Li_2SnO_3 appears while the amount of Sn dopant increases to 0.10. Fig. 3 demonstrates the dependence of lattice parameters a and c on x in $LiNi_{3/8}Co_{2/8}Mn_{3/8-x}Sn_xO_2$. With increase of Sn content from 0.00 to 0.05, a values increase linearly, while c value changes in the opposite direction. However, when $x = 0.10$, both a and c values are not on the line of linear relation, consistent with the XRD analysis, where it indicates that the secondary phase Li_2SnO_3 occurs when $x = 0.10$. Above results indicate that the phase-pure $LiNi_{3/8}Co_{2/8}Mn_{3/8-x}Sn_xO_2$ with a layered structure can be obtained in the range of $0 \le x \le 0.05$.

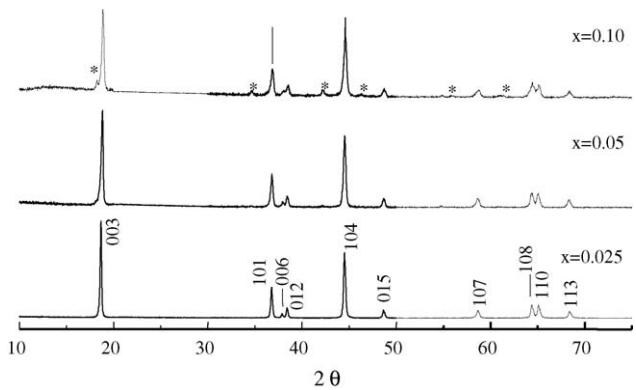

Fig. 2. XRD patterns of $LiNi_{3/8}Co_{2/8}Mn_{3/8-x}Sn_xO_2$ samples (*: Li_2SnO_3).

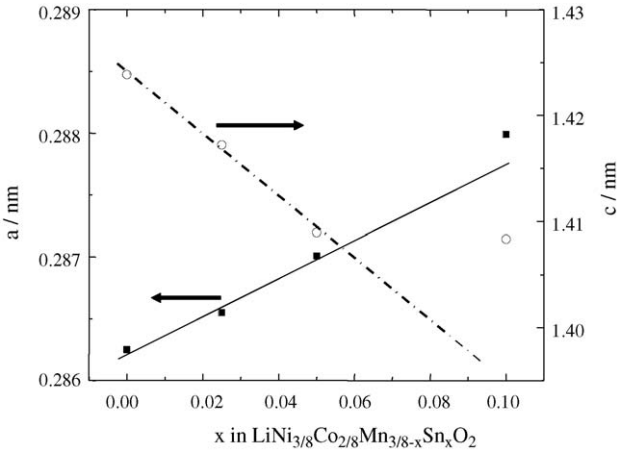

Fig. 3. The dependence of lattice parameters a and c on x in $LiNi_{3/8}Co_{2/8}Mn_{3/8-x}Sn_xO_2$.

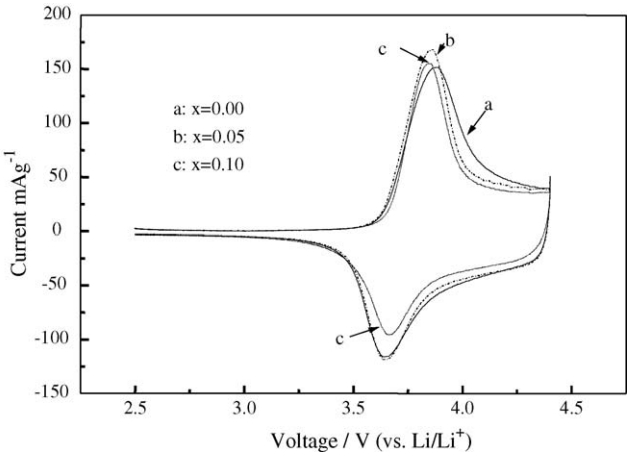

Fig. 5. Cyclic voltammograms for $LiNi_{3/8}Co_{2/8}Mn_{3/8-x}Sn_xO_2$ samples.

The integral intensity ratio of (0 0 3) to (1 0 4) lines (I_{003}/I_{104}) has been applied to measure the cation mixing in layered $LiMO_2$ (M: Co, Ni, Mn) compounds and a value of $I_{003}/I_{104} < 1.2$ is an indication of undesirable cation mixing [12,17]. A splitting of the lines assigned to the Miller indices (0 0 6), (1 0 2) and (1 0 8), (1 1 0) in the XRD patterns have also been considered to be characteristics of the layered structure [18,19]. In the case of un-doped sample, the ratio I_{003}/I_{104} is 1.47, indicating that it has higher degree of 2D order structure. Compared with the un-doped one, stannum doped samples with $x = 0.025$ and 0.05 exhibit similar I_{003}/I_{104} values and splitting between (0 0 6), (1 0 2) and (1 0 8), (1 1 0) doublet peaks, showing similar degree of 2D order structure while Sn dopant $x \leq 0.05$. However, the I_{003}/I_{104} value for the doped sample with $x = 0.10$ declines to 1.02, less than 1.20, indicating that large cation-mixing occurs in the sample.

The XRD analyses of as-prepared samples at different charge depth show that the crystal structure keep to be layered hexagonal phase during charging both for Sn doped and un-doped composite. Fig. 4 shows the change trend of the lattice parameters, indicating that the lattice parameters of doped sample have basically similar change trend as that of un-doped one during charging process.

The cyclic voltammogram (CV) curves of $LiNi_{3/8}Co_{2/8}Mn_{3/8-x}Sn_xO_2$ samples are shown in Fig. 5. Unlike $LiNiO_2$, which exhibits three sharp peaks in the CV curves due to three distinct phase transitions, $LiNi_{3/8}Co_{2/8}Mn_{3/8}O_2$ displays an oxidation peak centered at 3.88 V and a reduction peak centered at 3.64 V. Because no redox-reaction peaks near 3 V, corresponding to Mn^{3+}/Mn^{4+} redox reaction in layer-structured $Li_{2/3}(Ni_{1/3}Mn_{2/3})O_2$ [20], are observed and Co^{3+}/Co^{4+} redox reaction in layer-structured $Li(Ni_{1/3}Co_{1/3}Mn_{1/3})O_2$ [12] only occurs at 4.55–4.65 V, the couple of redox-reaction peaks is attributed to the redox reactions of Ni^{2+}/Ni^{4+} as speculated by Lu et al. [7]. All of other doped samples exhibit similar CV to that of the $LiNi_{3/8}Co_{2/8}Mn_{3/8}O_2$, but the oxidation peak declines and the reduction peak rises as Sn dopants increase. It is probably because Sn dopants can reduce the electrochemical impedance of $LiNi_{3/8}Co_{2/8}Mn_{3/8}O_2$.

The charge/discharge curves of samples are shown in Fig. 6. The discharge capacity of the un-doped sample is about 146 mAh g^{-1}. Compared with the un-doped one, doped samples with $x = 0.025$, 0.05 have enhanced discharge capacity of 151 and

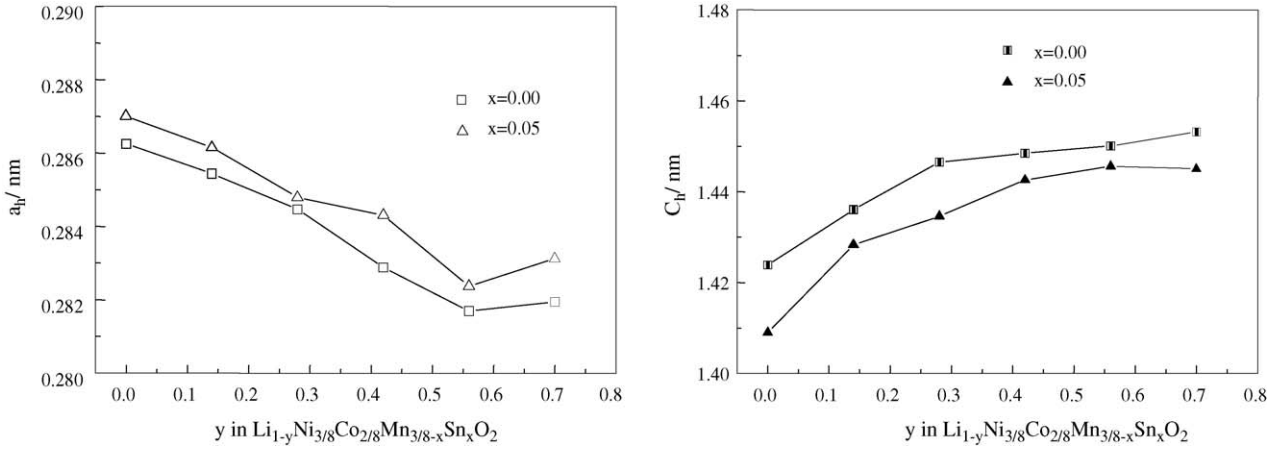

Fig. 4. Lattice constants of $Li_{1-y}Ni_{3/8}Co_{2/8}Mn_{3/8-x}Sn_xO_2$.

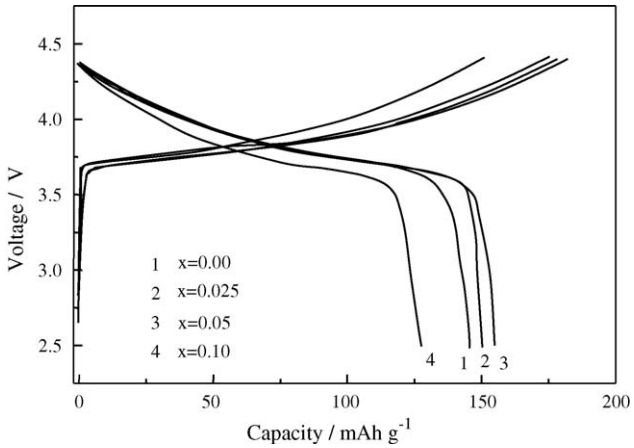

Fig. 6. Charge/discharge curves of the 3rd cycle for $LiNi_{3/8}Co_{2/8}Mn_{3/8-x}Sn_xO_2$ samples.

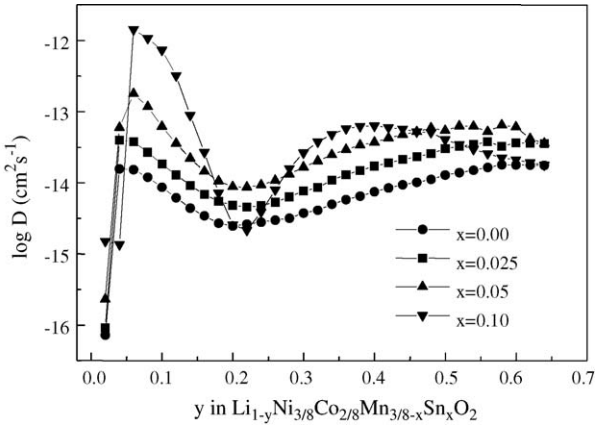

Fig. 8. Li^+ diffusion coefficient of $Li_{1-y}Ni_{3/8}Co_{2/8}Mn_{3/8-x}Sn_xO_2$.

156 mAh g^{-1}, respectively. It is probably caused by Sn doping, lowering the electrochemical impedance. However, the sample of $x = 0.10$ has only a discharge capacity of 127 mAh g^{-1}. As discussed previously, large cation-mixing and Li_2SnO_3 impure phase exist in the sample of $x = 0.10$ probably leads to its poorer electrochemical performance.

Fig. 7 demonstrates the dependence of discharge capacity of $LiNi_{3/8}Co_{2/8}Mn_{3/8-x}Sn_xO_2$ on the applied current densities. The capacity of the un-doped sample is 146.2 and 49.5 mAh g^{-1} at current density of 23 and 464 mA g^{-1}, respectively, indicating its poor rate capability. However, the rate capabilities and initial discharge capacities increase as Sn dopants increase in the range of $0 \le x \le 0.05$. The doped sample of $x = 0.05$ presents a capacity of 118.6 mAh g^{-1} at current density of 464 mA g^{-1}, corresponding to 76.3% of its capacity at 23 mA g^{-1}. Though the sample of $x = 0.10$ has a lower capacity of 129.1 mAh g^{-1} while discharged at 23 mA g^{-1}, it can present 83.2% of the capacity at current density of 464 mA g^{-1}, showing the best rate capability among the samples. Above results reveal that Sn doping is favorable to improve the rate capability of $LiNi_{3/8}Co_{2/8}Mn_{3/8}O_2$.

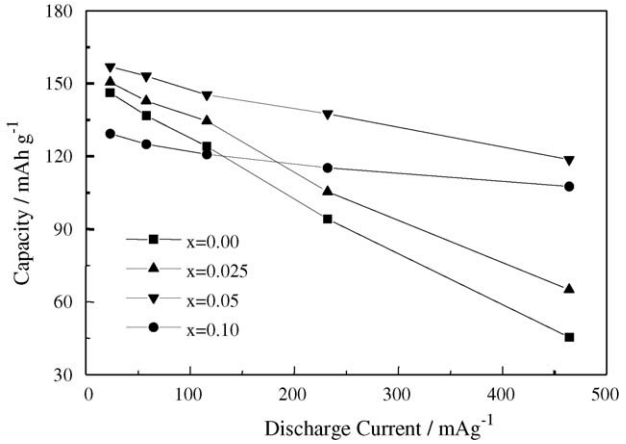

Fig. 7. Rate capability of $Li/LiNi_{3/8}Co_{2/8}Mn_{3/8-x}Sn_xO_2$ cells.

Effect of Sn doping on the chemical diffusion rate of Li^+ in $LiNi_{3/8}Co_{2/8}Mn_{3/8}O_2$ is investigated using GITT method. The variation of cell voltage on plotting against $t^{1/2}$ (t = time (s)) during the titration was seen to show straight-line behavior and the chemical diffusion coefficient of Li-ion, D_{Li}, is calculated according to the following equation derived by Weppner and Huggins [21]:

$$D_{Li} = \frac{4}{\pi}\left(\frac{V_M}{SF}\right)^2\left[I\left(\frac{\delta E}{\delta y}\right)\left(\frac{\delta E}{\delta t^{1/2}}\right)^{-1}\right]^2 \quad t \ll \tau \tag{1}$$

where V_M is the molar volume of sample (calculated from XRD results), S is the contact area between electrolyte and sample (calculated from the active material weight and its specific surface area), F is the Faraday constant, I is the applied constant electric current, $\delta E/\delta y$ is the slope of coulometric titration curves while $\delta E/\delta t^{1/2}$ is the slope of the short-time transient voltage change. The equation is valid for times shorter than the diffusion time $\tau = (d/2\pi)^2(1/D)$ where d is the average diameter of grains.

Fig. 8 demonstrates the chemical diffusion coefficients as a function of y in $Li_{1-y}Ni_{3/8}Co_{2/8}Mn_{3/8-x}Sn_xO_2$ by substitution of the $\delta E/\delta y$ and $\delta E/\delta t^{1/2}$, calculated for different values of y in Eq. (1). The un-doped sample is found to have the chemical diffusion coefficient ranging from 2.54×10^{-15} to 1.34×10^{-14} cm s^{-1}. The chemical diffusion coefficients are enhanced as Sn dopants increase. The doped sample with $x = 0.05$ possesses higher chemical diffusion coefficient by almost one order of magnitude than the un-doped one, which result in lower electrochemical reaction impedance, leading to better rate capability and more discharge capacity.

The cycleabilities of samples are shown in Fig. 9. All samples exhibit stable discharge capacity. The discharge capacity of the un-doped sample is about 146 mAh g^{-1}. Compared with the un-doped one, the discharge capacities of doped samples with $x = 0.025$ and 0.05 are enhanced to be 151 and 156 mAh g^{-1}, respectively. However, the sample of $x = 0.10$ has only a discharge capacity of 127 mAh g^{-1}. Therefore, the doping Sn should be proper.

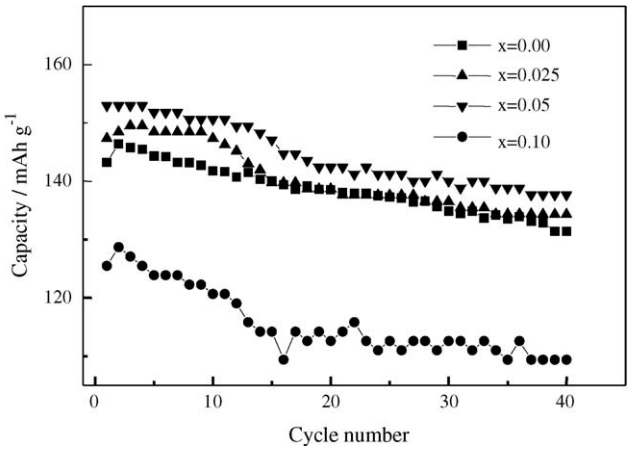

Fig. 9. Cycleabilities of Li/$LiNi_{3/8}Co_{2/8}Mn_{3/8-x}Sn_xO_2$ cells.

Fig. 9 also shows that the Sn doping has little effect on cycleability. Therefore, the proper doping of Sn can enhance the rate capability of $LiNi_{3/8}Co_{2/8}Mn_{3/8}O_2$, but no improvement to its cycleability.

4. Conclusions

$LiNi_{3/8}Co_{2/8}Mn_{3/8-x}Sn_xO_2$ ($0 \le x \le 0.10$) was prepared and characterized by Sn^{4+} substituting for Mn^{4+}. The compound remains single-phase layered structure within a range of $0 \le x \le 0.05$, and shows improved discharge capacity and rate capability as Sn dopants increase. The sample with $x = 0.10$ has the best rate capability of all the presented samples, but its discharge capacity reduces markedly due to secondary phase Li_2SnO_3 and increase of cation-disordering. The compound of $x = 0.05$ shows optimum cathodic behaviors in view of discharge capacity and rate capability. The Sn doping is favorable to improve the rate capability of $LiNi_{3/8}Co_{2/8}Mn_{3/8}O_2$. It is a promising alternative cathode material for EV application of Li-ion batteries.

Acknowledgment

The authors highly appreciate the financial support from Chinese National Funded High Technology Research Project (863 project), Grant No. 2002AA323020 and No. 2002AA501832.

References

[1] T. Iwahori, Y. Ozaki, A. Funahashi, H. Momose, I. Mitsuishi, S. Shiraga, S. Yoshitake, H. Awata, J. Power Sources 81–82 (1999) 872.
[2] M. Broussely, J. Power Sources 81–82 (1999) 140.
[3] T. Tanaka, K. Ohta, N. Arai, J. Power Sources 97–98 (2001) 2.
[4] Y. Nishi, J. Power Sources 100 (2001) 101.
[5] X.M. He, J.J. Li, Y. Cai, Y.W. Wang, J.R. Ying, C.Y. Jiang, C.R. Wan, J. Solid State Electrochem. 9 (2005) 438.
[6] D.D. MacNeil, Zh. Lu, Zh. Chen, J.R. Dahn, J. Power Sources 108 (2002) 8.
[7] Zh. Lu, D.D. MacNeil, J.R. Dahn, Electrochem. Solid-State Lett. 4 (2001) A191.
[8] T. Ohzuku, Y. Makimura, Chem. Lett. (2001) 744.
[9] S.H. Kang, J. Kim, M.E. Stoll, D. Abraham, Y.K. Sun, K. Amine, J. Power Sources 112 (2002) 41.
[10] Zh. Lu, D.D. MacNeil, J.R. Dahn, Electrochem. Solid-State Lett. 4 (2001) A200.
[11] J.S. Kim, C.S. John, M.M. Thackeray, Electrochem. Commun. 4 (2002) 205.
[12] K.M. Shaju, G.V. Subba Rao, B.V.R. Chowdari, Electrochim. Acta 48 (2002) 145.
[13] J.G. Li, C.R. Wan, D.P. Yang, Z.P. Yang, Acta Phys. Chim. Sin. 19 (2003) 1030.
[14] J.G. Li, C.R. Wan, D.P. Yang, Z.P. Yang, J. Inorg. Mater. 19 (2004) 1298.
[15] S.-H. Kang, K. Amine, J. Power Sources 124 (2003) 533.
[16] L. Zhang, K. Takada, N. Ohta, et al., Mater. Lett. 58 (2004) 3197.
[17] T. Ohzuku, A. Ueda, M. Nagayama, Y. Iwakoshi, H. Komori, Eletrochem. Acta 38 (1993) 1159.
[18] A. Rougier, P. Gravereau, C. Delmas, J. Electrochem. Soc. 143 (1996) 1168.
[19] R. Moshtev, P. Zlatilova, V. Manev, et al., J. Power Sources 62 (1996) 59.
[20] J.M. Paulsen, C.L. Thomas, J.R. Dahn, J. Electrochem. Soc. 147 (2000) 861.
[21] W. Weppner, R.A. Huggins, J. Electrochem. Soc. 124 (1977) 1569.